Natural Resources Canada | Ressources naturelles Canada

GEOLOGICAL SURVEY OF CANADA
OPEN FILE 8804

Mineralogy of mudstone, bocanne, and klinker deposits, Smoking Hills (Ingniryuat), Northwest Territories, Canada

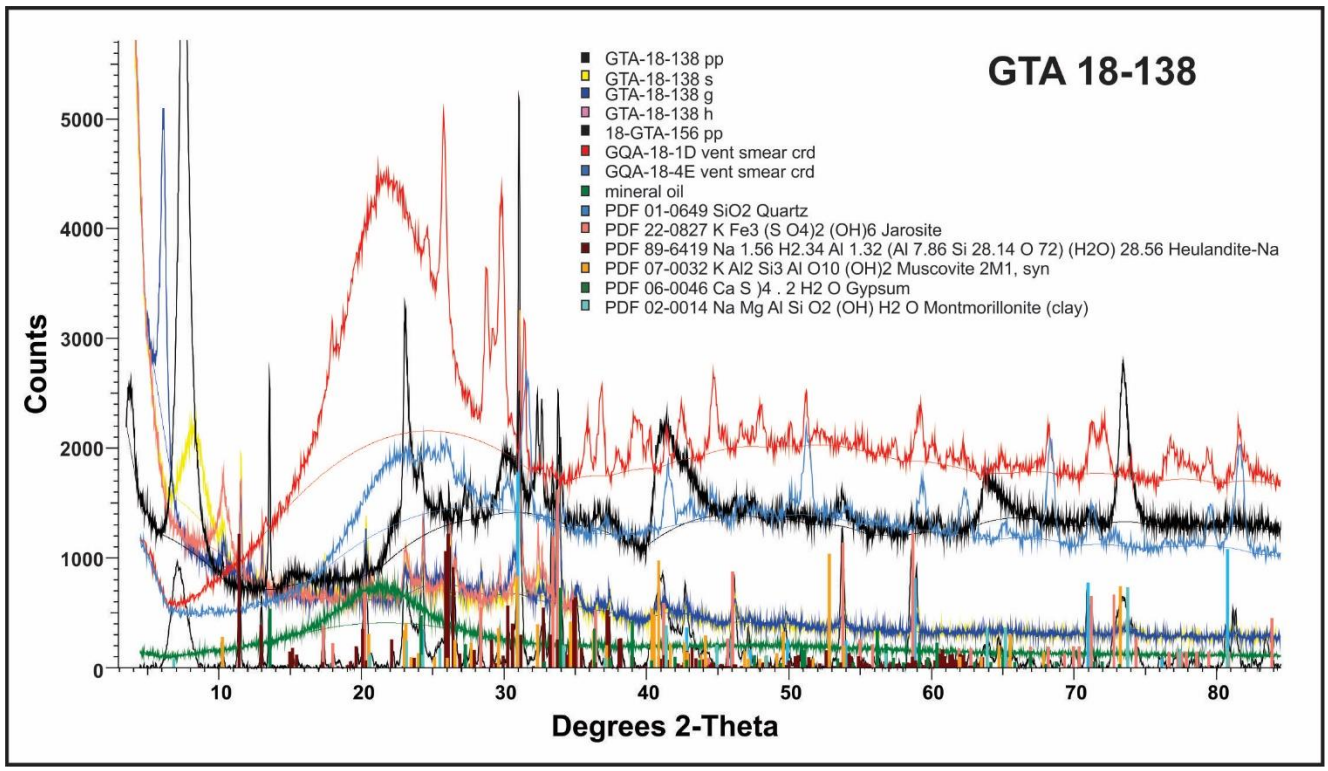

J.B. Percival, I. Bilot, T. McLoughlin-Coleman, S.E. Grasby, and M.J. Polivchuk

2021

Canada

GEOLOGICAL SURVEY OF CANADA
OPEN FILE 8804

Mineralogy of mudstone, bocanne, and klinker deposits, Smoking Hills (Ingniryuat), Northwest Territories, Canada

J.B. Percival[1], I. Bilot[1], T. McLoughlin-Coleman[2], S.E. Grasby[3], and M.J. Polivchuk[1]

[1]Geological Survey of Canada, 601 Booth Street, Ottawa, Ontario
[2]Department of Earth Sciences, Carleton University, 1125 Colonel By Drive, Ottawa, Ontario
[3]Geological Survey of Canada, 3303 33rd Street Northwest, Calgary, Alberta

2021

Permanent link: https://doi.org/10.4095/328476

This publication is available for free download through GEOSCAN (https://geoscan.nrcan.gc.ca/).

Recommended citation

Percival, J.B., Bilot, I., McLoughlin-Coleman, T., Grasby, S.E., and Polivchuk, M.J., 2021. Mineralogy of mudstone, bocanne, and klinker deposits, Smoking Hills (Ingniryuat), Northwest Territories, Canada; Geological Survey of Canada, Open File 8804, 1 .zip file. https://doi.org/10.4095/328476

Publications in this series have not been edited; they are released as submitted by the author.

ABSTRACT

Combusting mudstones in the Smoking Hills area, Northwest Territories, were reported by European Arctic explorers in the early part of the 19th century. These sites emit hot sulphuric gases due to auto-combustion of pyrite-rich zones. The acidic gases react with the surrounding mudstones to precipitate brightly coloured mineral deposits. In this study, samples were collected from active burning sites (bocanne), inactive sites (klinker) and unaltered mudstones to characterize their mineralogy. The active sites are comprised of variable amounts of discrete sulphate minerals from seven different mineral groups, whereas the inactive sites are characterized mainly by jarosite, gypsum and quartz. The mudstone mineralogy shows most samples contain variable amounts of quartz, muscovite/illite, heulandite and jarosite and a host of other minerals in minor to trace amounts. Understanding the mineralogy of these sites provides new insights on formation of high-temperature acid minerals.

Frontispiece: Diffractograms of bocanne samples showing mineral oil peak (very broad) and method of smoothing applied to the various samples and treatments.

TABLE OF CONTENTS

LIST OF FIGURES

LIST OF TABLES

Tables are hyperlinked in the document, see readme file for how to access.

1. INTRODUCTION

The Smoking Hills are an upland region extending from Franklin Bay to the Anderson River (Fig. 1). Known as Ingniryuat by the Inuvialuit, they were first recorded in the literature by Sir John Richardson of the second Franklin overland expedition (Richardson, 1828). The name is derived from auto-combustion of organic rich Cretaceous mudstones (the Smoking Hills Formation) that emit large clouds of smoke. Such burning mudstones are termed "bocannes" (Selwyn, 1877; Crickmay, 1967) and are characterised by emissions of hot sulphuric gases from vent holes surrounded by brightly coloured mineral deposits (Fig. 2). Sites that are no longer venting gas are common in the region, and are characterised by brick red to yellow deposits known as "klinkers". Both burning and extinct sites are observed over a wide area of the Anderson Plain region and are directly associated with outcrop of the Smoking Hills Formation (Yorath et al., 1975; Yorath and Cook, 1981). Work by Mathews and Bustin (1984) suggest the burning is associated with oxidation of pyrite as well as combustion of organic matter in the mudstones. The calorific heat value is estimated to be up to 4000 kJ/kg. Their detailed work corroborates initial suggestions of Richardson (1828) as well as Dawson (1881; working in related strata in north and central Alberta).

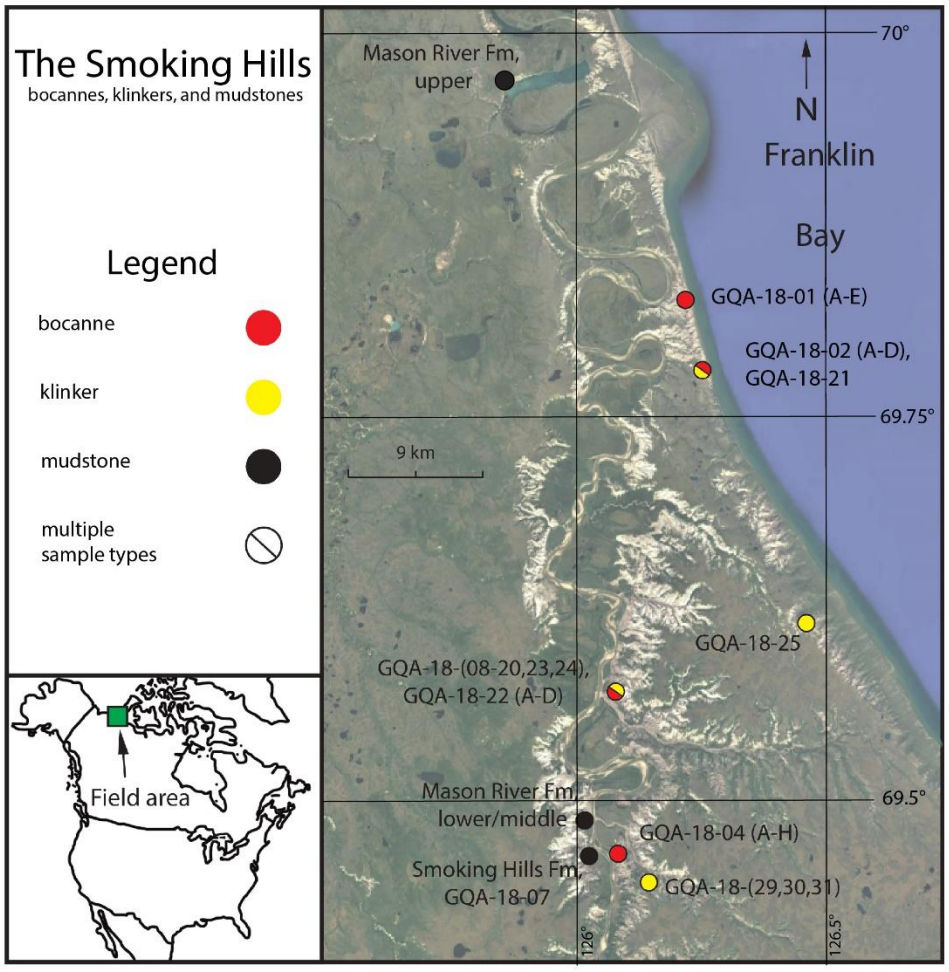

Fig. 1. Location map of selected samples for XRD analyses from Smoking Hills area, NWT. Google Earth Image with permission.

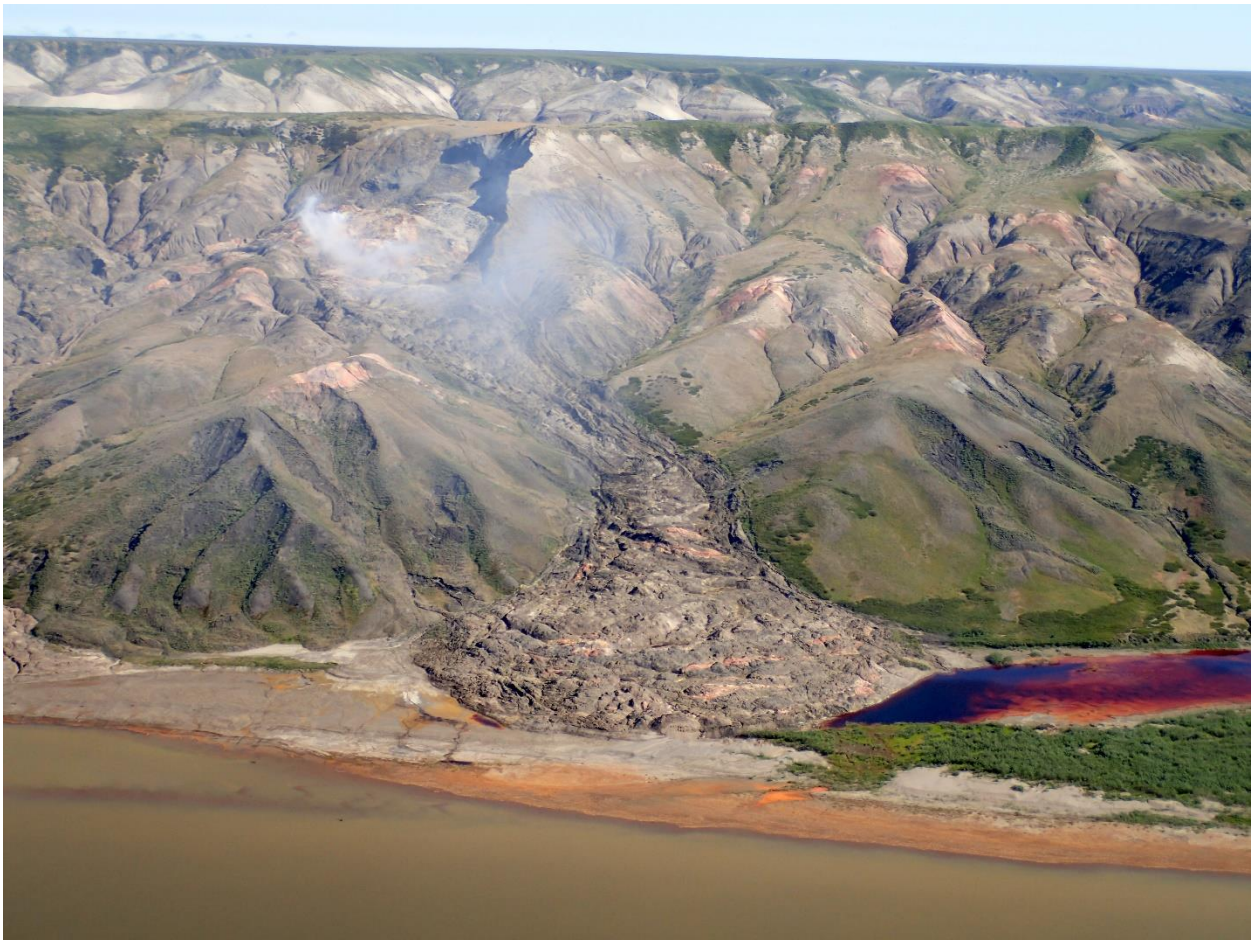

Fig. 2. View (looking east) of the Smoking Hills jarosite-rich materials (orange) and acidic iron-rich waters (red) due to leaching from slumping mudstone (photographer Dr. Rod Smith, July 29, 2018; NRCan photo 2021-137).

This study forms part of a larger project investigating the Cretaceous bedrock in Canada's Arctic, under the Geo-Mapping for Energy and Minerals (GEM-II) Program, Western Arctic Margins project. The focus of one of the main activities was to understand the bocanne mineralogy and hydrochemistry in the Smoking Hills area (Smith et al., 2018), which will provide new insights into formation of high-temperature acidic minerals.

2. METHODS

2.1 Sample Selection

Three suites of samples were submitted for detailed mineralogical characterization. These include mudstone samples, klinker samples formed though thermal alteration of organic-rich mudstones, and bocanne samples collected near vents of active burning sites in the Smoking Hills (Fig.1). At any site, grab samples that represent the full visible range of colour and mineral morphology observed were placed in Falcon™ tubes. As precipitated samples were noted to actively effloresce following collection, an effort was made to preserve them by immediate submersion in mineral oil (Johnson's® baby oil). At klinker sites, samples were similarly collected to represent the range of colours and textures/morphologies present. Additional samples of the unburnt mudstone were also collected from the stratotype of the Smoking Hills Formation (Yorath et al., 1975). For comparison, samples from the overlying Mason River Formation were also assessed for mineralogical content. Details on sample location, rock type and initial sample preparation is provided in Table A1 of Appendix A.

2.2 X-ray Diffraction Analysis

The mineralogy of bulk materials was determined by X-ray powder diffraction analysis (XRD) in the GSC mineralogy lab. Bulk samples were micronized using a McCrone mill (now XRD-Mill McCrone – RETSCH Micronizing Mill) in isopropyl alcohol until a grain size of about 5-10 µm was obtained. The samples were air-dried and then back-pressed into an aluminum holder to produce a randomly-oriented specimen. For some select samples, oriented (smear) mounts were made to differentiate the clay minerals and determine if smectite was present. The smears were made by suspending 40 mg of material in distilled water, mixing thoroughly with a Vortex mixer (Fisher Scientific Genie 2), and then pipetted onto glass slides and air-dried overnight. X-ray patterns were recorded on a Bruker D8 Advance Powder Diffractometer equipped with a Lynx-Eye Detector, Co Kα radiation set at 35 kV and 35 mA. The smears were analysed air-dried, then after glycol saturation followed by heat treatment (550 EC for 2 hours).

2.2.1 Mineral Identification and Quantitative Analysis

Initial identification of minerals was made using EVA (Bruker AXS Inc.) software with comparison to reference mineral patterns using Powder Diffraction Files (PDF) of the International Centre for Diffraction Data (ICDD) and other available databases. Quantitative analysis was carried out using TOPAS (Bruker AXS Inc.), a PC-based program that performs Rietveld refinement (RR) of XRD spectra, based on a whole pattern fitting algorithm. Quantitative results are more precise if mineralogical structure files (.cif) match the unknown as close as possible.

Quantitative analyses appear reasonable when minerals in the samples are matched to the standards. The lower the Goodness of Fit (GoF) value (i.e., generated by TOPAS for the whole pattern; best fit closer to 1), the better the standards match the unknowns and the more confident are the results. Difficulty arises when clay minerals of varying composition (e.g., expandable layers, mixed-layers) are encountered, or when mineral species have overlapping X-ray peaks

(e.g., kaolinite and chlorite; quartz and graphite). Also, there are a limited number of reference minerals available as structure files so there may not be an exact match to the mineral being analyzed (e.g., using actinolite rather than ferro-hornblende). Differences in quantification will also arise if using a pressed powder (preferable for RR) vs. smear (oriented) samples.

2.2.2 Semi-Quantitative Analysis

For some samples (e.g., samples coated in oil or prepared as smears), only semi-quantitative analyses are provided. These results are based on the Reference Intensity Ratio (RIR) method (EVA software; Bruker AXS, Inc.). The RIR method uses corundum as an internal standard such that the most intense X-ray peak for each mineral phase is compared to the 100% intensity corundum peak (i.e., I/Ic). These constants are collected and recorded in the ICDD-PDF files of each reference mineral. The software allows iterative comparisons between the unknown sample and the reference minerals in the PDF database.

2.3 Cleaning of Oil-Saturated Samples

The bocanne samples were collected in the field and placed in 50-mL Falcon™ containing mineral oil. The amount of oil used unfortunately saturated the samples. In order to examine them in more detail, the oil was removed by washing in isopropyl alcohol. The non-fragile samples were broken into small pieces, placed in a 15 mL centrifuge tube and filled half-way with alcohol. The samples were agitated using a Vortex mixer for about one minute. If the sample was more fragile, or showed an unusual texture or structure, it was placed in a weighing boat, covered in isopropyl alcohol, and swirled gently for ~30 seconds to remove excess oil. The samples were then placed in a clean weighing boat and allowed to dry under a heat lamp.

In order to make mineral identifications easier, an individual mineral or grain was plucked out from the oil, allowed to drip back into the sample vial, and placed in a mortar for grinding. The oily paste was scraped into a 15-mL centrifuge tube and ~5 mL of isopropyl alcohol was added. The mixture was agitated using the Vortex mixer for about 30 seconds. The suspension was then pipetted onto a zero background plate and left to dry for approximately 5 minutes under a heat lamp. The sample was run immediately on the XRD once the alcohol had evaporated, using a rapid scan (~ 7 minutes). This prevented de-hydration of the samples in air. In addition, sample mounts were used for detailed examination under a binocular microscope (Olympus SZH10 with variable magnification equipped with a Lumenera Infinity 2 digital camera) or the Zeiss EVO SEM.

2.4 SEM Analysis

Grain mounts were examined under a Zeiss EVO 50 series Scanning Electron Microscope (SEM) with Extended Pressure capability (up to 3000 pascals). The SEM is equipped with a Backscattered Electron Detector (BSD), Everhart -Thornley Secondary Electron Detector (SE), Variable Pressure Secondary Electron Detector (VPSE), and a Cathodoluminescence Detector (CL). Elemental analyses were acquired using an Oxford EDS system (energy dispersive spectroscopy) comprised of a X-Max 150 Silicon Drift Detector and AZtec Energy 4.1 microanalysis software. SEM

operating conditions include a working distance of 8.5 mm, high voltage (EHT) set at 20 kV, probe current set at 400pA to 1nA and filament current set to the 2nd peak. Samples were analysed in variable pressure mode using a chamber pressure of approximately 70 Pa.

3. RESULTS

In this study, 38 different minerals were identified including 24 unique sulphate minerals. Those identified and their symbols and formulas are given in Table 1. Note that in the zeolite group, heulandite and clinoptilolite form a solid solution series and are difficult to differentiate using XRD analysis. For convenience, the mineral is labelled as heulandite (either the Ca or K variety) in the results tables.

3.1 Mudstone Samples

Forty mudstone samples were selected for mineralogical analyses. These included one suite of 24 collected from the Smoking Hills Formation, another suite of 11 from the overlying Mason River Formation, four KUS (map code for Cretaceous – Upper – Smoking Hills Formation) Smoking Hills Formation mudstones that were soaked in distilled water to observe any geochemical changes that may occur, and one concretion from a bedrock raft within glacial sediments (Evans et al., in press). Results for the Smoking Hills Formation are given in Table 2 and the remaining mudstone samples in Table 3 and Table 4, respectively. Summary statistics (detectable in 3 or more specimens) are given in Table 5. Samples in the grey boxes were freeze-dried in the GSC-Ottawa Sedimentology Laboratory prior to pulverization. All samples were pulverized in the McCrone micronizing mill to prepare pressed powder mounts. All samples (Tables 2-4, column %XL) are poorly crystalline with an amorphous content ranging from 10 to 90 wt.% with a mean slightly greater than 50 wt.%.

3.2 Smoking Hills Formation

For the Smoking Hills Formation suite, there are four slightly weathered mudstone samples (sample numbers in italics) and three samples labelled with asterisks that pertain to layers with special features. These include GTA 18-135* as jarosite-bearing, GTA 18-138* as jarosite- and bentonite-rich, and GTA 18-183 as jarosite-rich. In general, the samples from this locality are black bituminous mudstone with abundant jarosite bands.

All samples (n = 21) contain abundant to minor quartz (mean = 22.5 wt.%) and gypsum (mean = 5.4). Note the astericks-labelled samples were not included in the statistical analyses. Nearly all samples contain abundant to minor heulandite (n = 17, mean = 23 wt.%), mica (muscovitic; n = 18, mean = 14.5 wt.%), and jarosite (combined; n = 20, mean = 21.9 wt.%). Three different jarosite structures fit the data, but for statistics, they were combined as one set. About half the samples, with a few exceptions, contain minor to trace amounts of plagioclase feldspar (two samples abundant), smectite (two samples abundant) and alunogen. The presence of alunogen is not completely confirmed, as it is under the mica 10 Å X-ray peak. Verification using polished thin

sections would be useful. Some of the samples contain minor to trace chlorite, kaolinite, tamarugite and K-feldspar. The goodness of fit is good with a mean value of 2.5. The slightly weathered mudstone samples do not appear to be different in terms of their mineralogy, except for KUS 18-532 which is sulphate-rich and quartz-poor. In all, eight different sulphate minerals were identified, however, jarosite and gypsum are the most common.

An example of the search/match using EVA software (Bruker AXS, Inc.) for one of the weathered mudstones is shown in Figure 3. This sample (SUV 18-532) consists of abundant sulphate minerals including tamarugite and halotrichite, as well as minor gypsum and jarosite. The quantitative results from TOPAS (Bruker AXS, Inc.) is shown in Figure 4. Here you can see the amorphous nature of the sample (only 13% crystalline) with the rising background of the diffractogram. In Figure 3, the background has been removed which allows easier identification and matching to reference minerals.

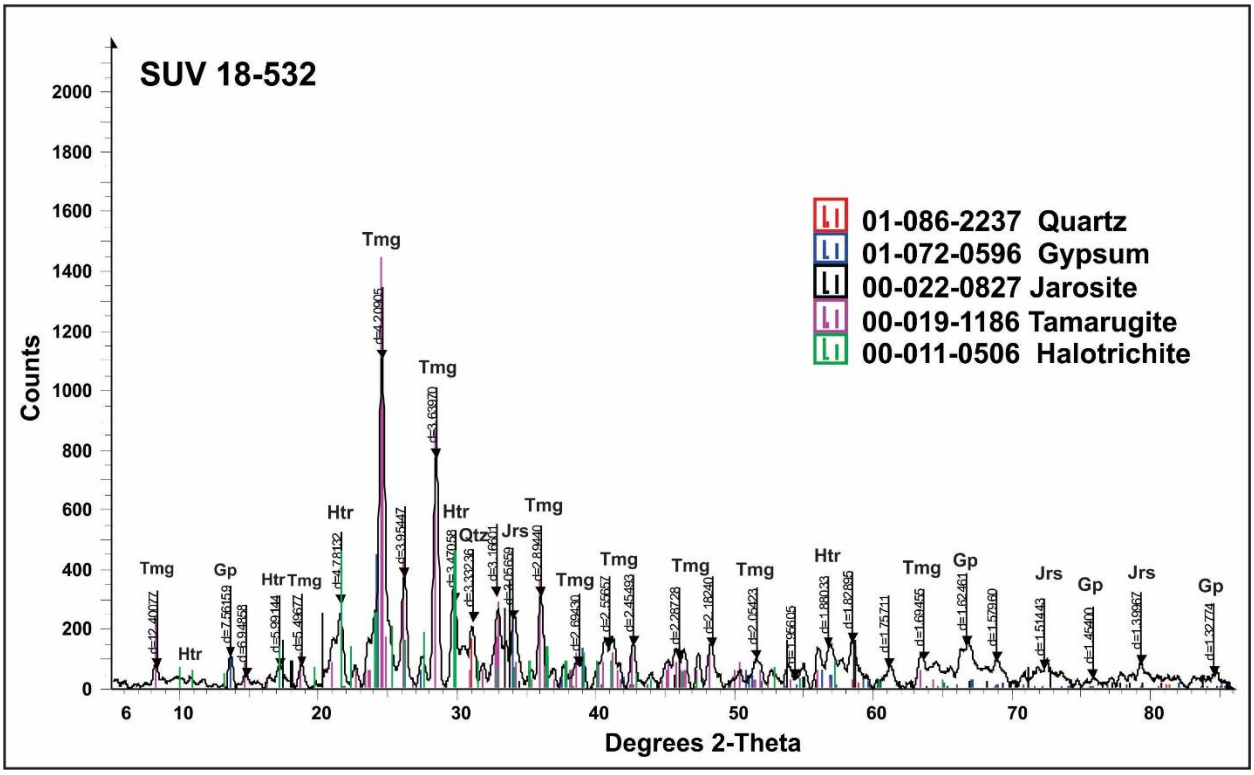

Fig. 3. Search/Match using EVA software (Bruker AXS, Inc.) for sample SUV 18-532, slightly weathered mudstone (Gp: gypsum, Htr: halotrichite, Jrs: jarosite, Qtz: quartz, Tmg: tamarugite).

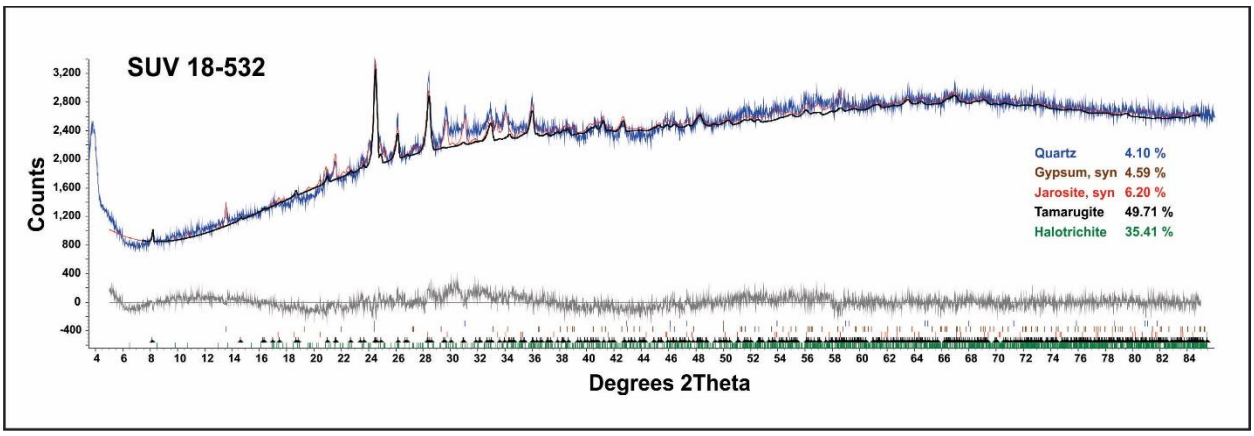

Fig. 4. Quantitative analysis by RR using TOPAS software (Bruker AXS, Inc.) for sample SUV 18-532, slightly weathered mudstone (Gp: gypsum, Htr: halotrichite, Jrs: jarosite, Qtz: quartz, Tmg: tamarugite). Note amorphous content evident in rising background of diffractogram.

The search/match for one of the special selected layers, sample GTA 18-138*, is shown in Figure 5. This sample was described as a bentonite and jarosite-rich layer. However, although jarosite is present, smectite is most abundant (67 wt.%). Figure 6 shows the quantitative results based on TOPAS-RR analyses. Note this sample is more crystalline (54 wt.%) and the rise in the background on the diffractogram is much less pronounced than shown in Figure 4. To show the abundance of smectite, a sub-sample was mounted as a smear (oriented). The stacked diffractograms for air-dried, glycol-saturated and heated runs are shown in Figure 7. Note the intense ~16.7 Å X-ray peak for smectite in the glycol-saturated diffractogram (red) and the collapse to 10 Å after heat treatment. The sulphate minerals are affected (destroyed) by the heat treatment. Alunogen is under the smectite and mica X-ray peaks.

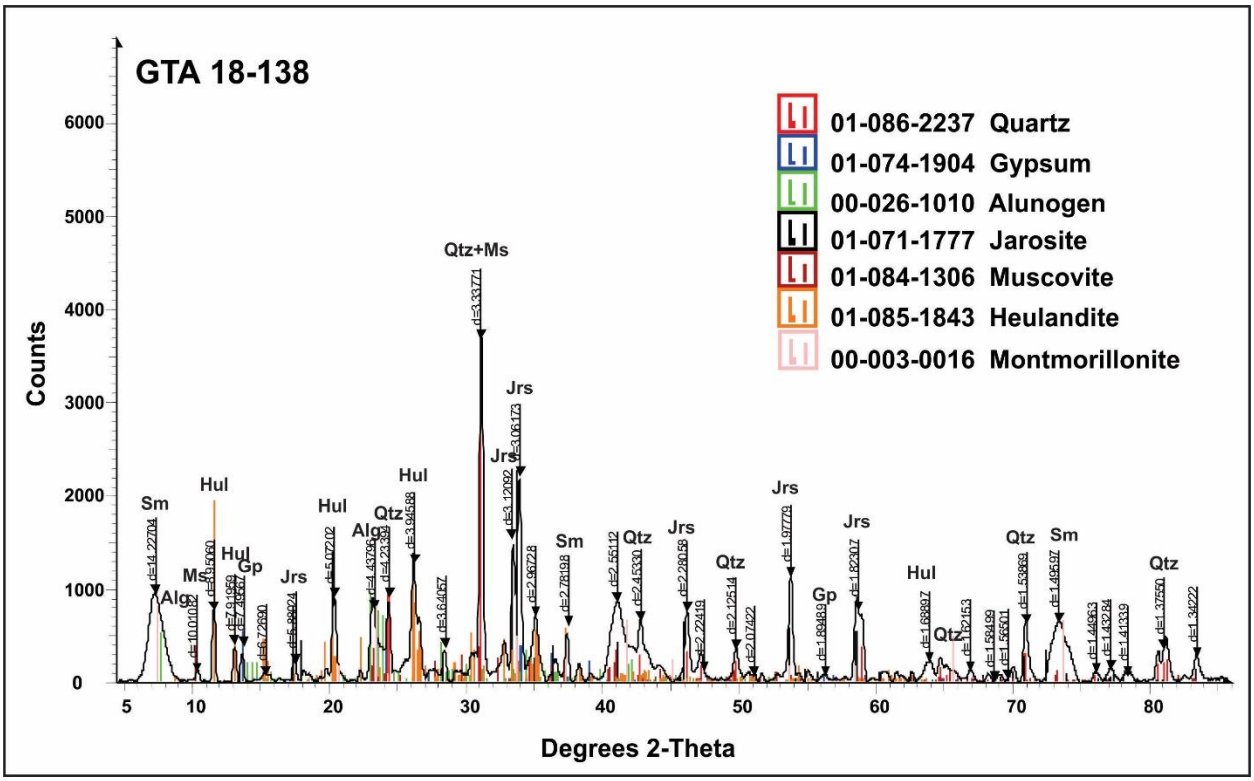

Fig. 5. Search/Match using EVA software (Bruker AXS, Inc.) for sample GTA 18-138, mudstone (Alg: alunogen, Gp: gypsum, Hul: heulandite, Jrs: jarosite, Ms: muscovite, Qtz: quartz, Sm: smectite (montmorillonite).

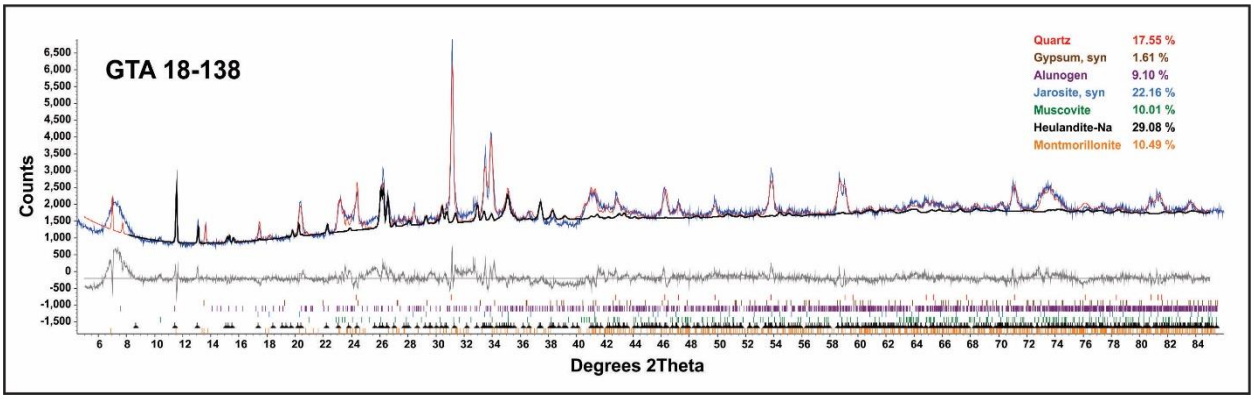

Fig. 6. Quantitative analysis by RR using TOPAS software (Bruker AXS, Inc.) for sample GTA 18-138.

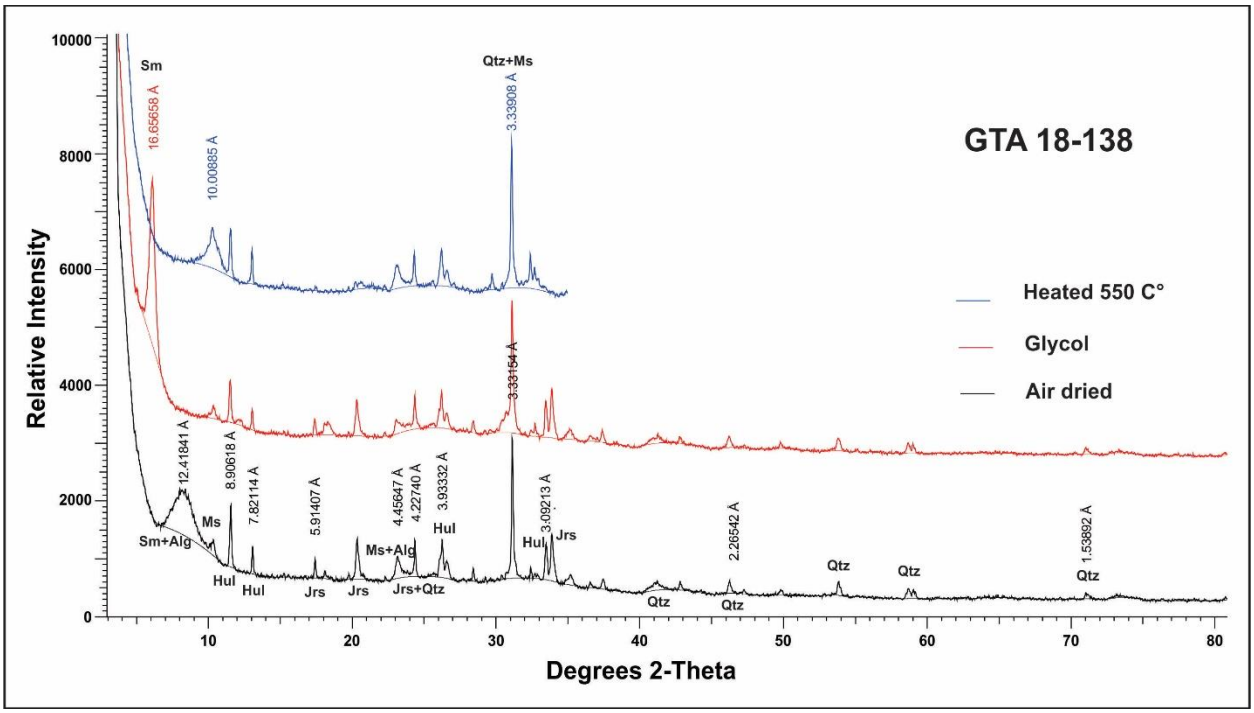

Fig. 7. Stacked diffractograms for sample GTA 18-138 for air-dried, glycol saturated and heat-treated smear mount. Note the distinctive smectite (or ML) at 16. 7 Å X-ray peak after glycolation; gypsum not detected (Alg: alunogen, Hul: heulandite, Jrs: jarosite, Ms: muscovite, Qtz: quartz, Sm: smectite (montmorillonite)).

Variations in mineralogy are plotted relative to stratigraphic height as measured in outcrop in Figure 8. The samples were collected from the stratotype section of the Smoking Hills Formation, starting at 3 m from the base of the formation up to a height of 77.5 m at the formation's upper contact. For simplicity, some mineral phases were combined including: quartz + cristobalite, plagioclase feldspar + K-feldspar, all phyllosilicates, and all sulphate minerals. It is evident that throughout the stratigraphic section the mineralogy is variable, however, the presence of sulphate minerals increases towards the lowest stratigraphic layer. Feldspar minerals are nearly absent at the top and bottom of the section, but present in minor amounts in some layers. Heulandite, a zeolite group mineral is relatively abundant in many layers throughout the section. As sulphate mineral content increases in the lower parts, feldspar, heulandite and phyllosilicate minerals are nearly absent. Quartz with minor to trace cristobalite tend to be abundant throughout with a few exceptions.

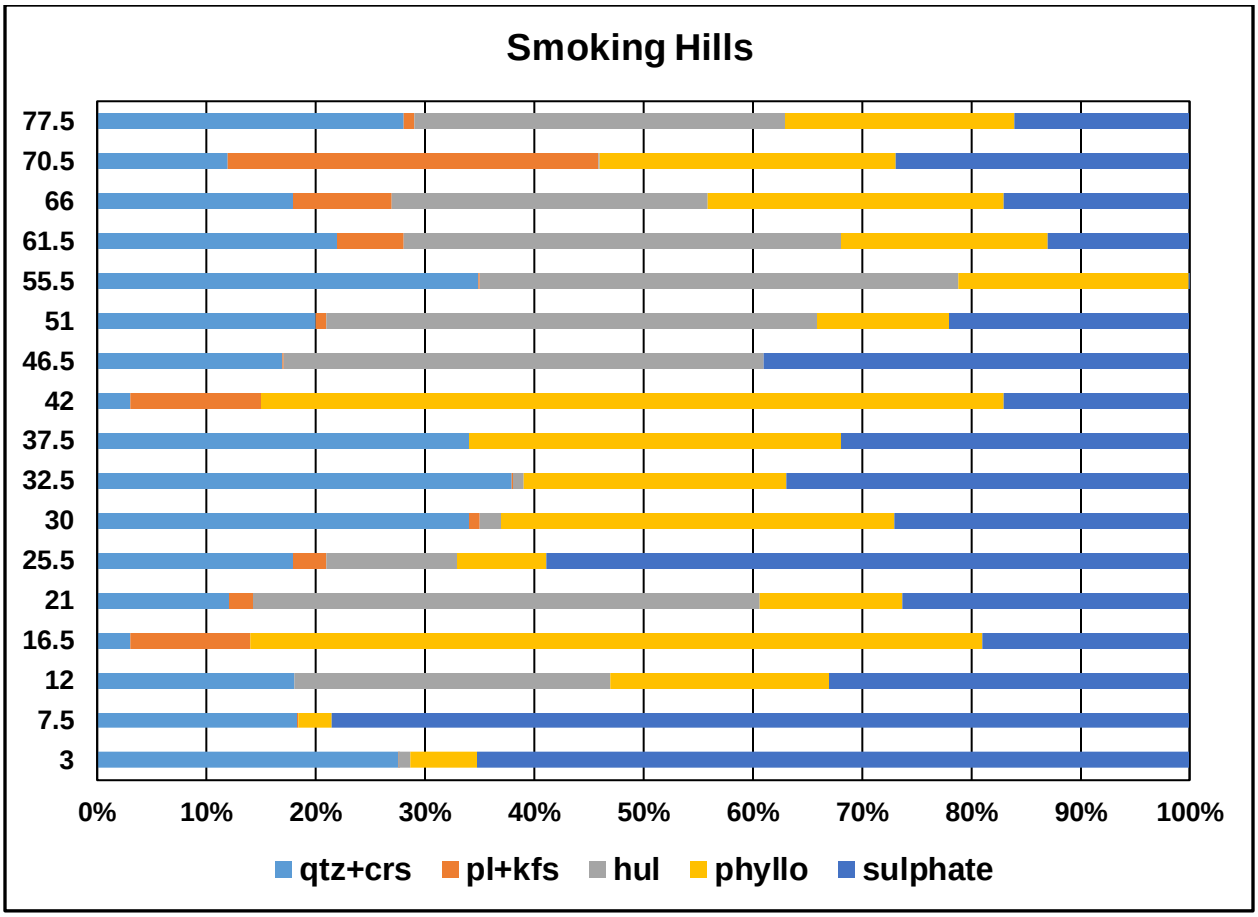

Fig. 8. Variation of major mineral phases (wt.%) with depth (metres from base of the formation) for mudstone samples, from the Smoking Hills type section (69°27'52":W126°58'13").

Variation with depth for the individual mineral phases are given in Figure 9. For the major silicates, when quartz and heulandite content decreases, the total feldspar content increases. Note the heulandite concentration in some layers is very high, up to 45 wt.%. With regard to the phyllosilicates, muscovitic mica and smectite tend to be more prevalent throughout the section relative to chlorite and kaolinite; note the large increase in smectite at 32.5 m (60 wt.%). This represents an ash layer in this section. The sulphate minerals alunogen, gypsum and jarosite are also plotted in Figure 9 with jarosite as a combination of the three species identified (see Table 2). Although it shows sulphate minerals increasing with depth, it is evident that jarosite is the main reason due to their abundance. Although no pyrite was detected in these samples, the presence of jarosite indicates that oxidation of sulphides has occurred. According to Michel and van Everdingen (1987), jarosite is precipitated from acidic iron-bearing groundwater seeps in Cretaceous shales in the Tulita (Fort Norman) area (NWT).

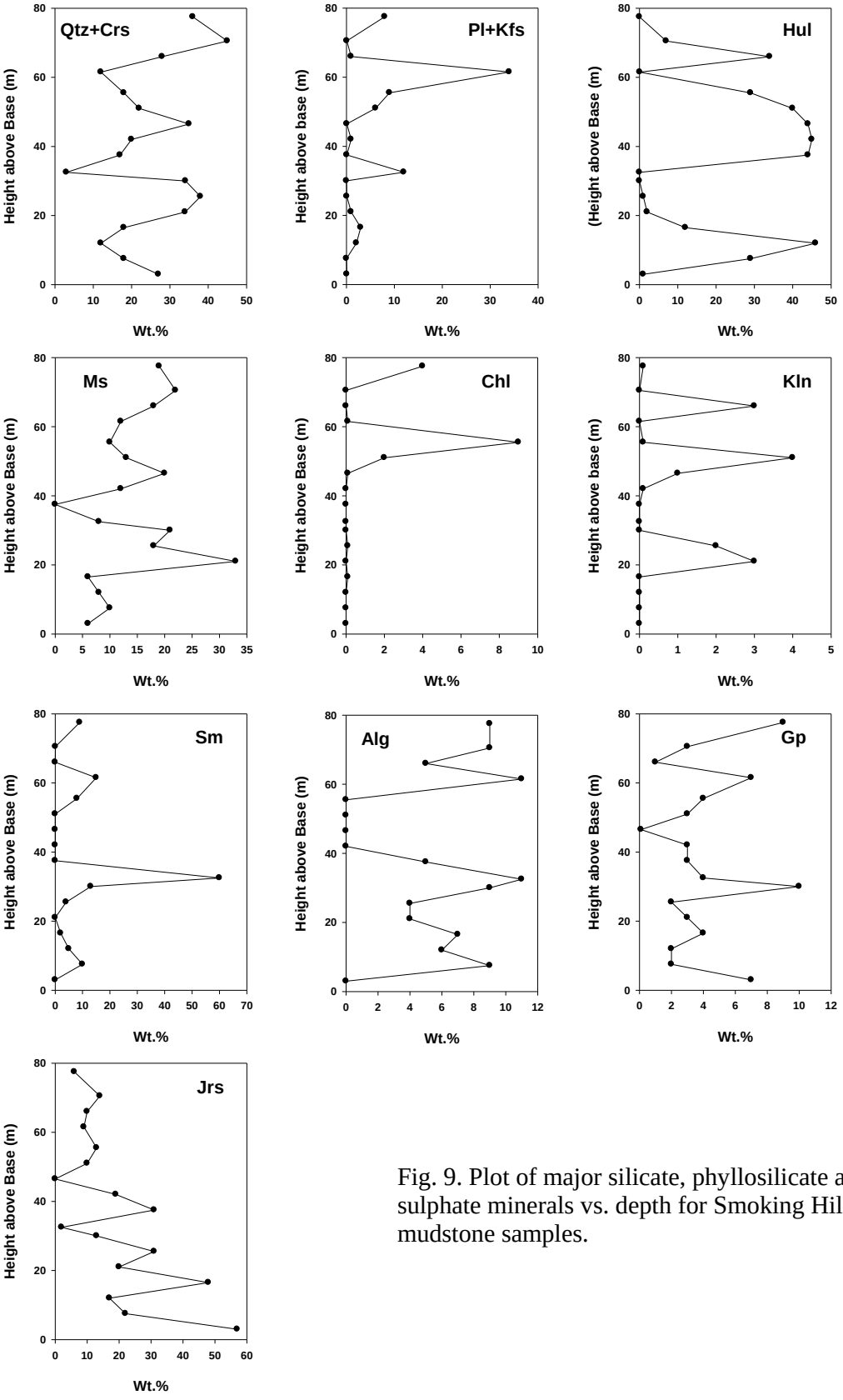

Fig. 9. Plot of major silicate, phyllosilicate and sulphate minerals vs. depth for Smoking Hills mudstone samples.

3.3 Mason River Formation

The mineralogy of the overlying Mason River Formation (Table 3) is slightly different than the Smoking Hills Formation units. The samples contain abundant to minor quartz (mean = 28.5 wt.%), mica (muscovitic; mean = 18.5 wt.%), minor alunogen (mean = 12.9 wt.%), plagioclase feldspar (mean = 10.6 wt.%), kaolinite (mean = 9.0 wt.%), chlorite (mean = 8.7 wt.%) and smectite (mean = 7.1 wt.%), and minor to trace K-feldspar, jarosite, gypsum and cristobalite. In these units, four different sulphates were identified, and alunogen needs to be verified. The goodness of fit is good with a mean of 2.9.

Variation with depth of the undivided Middle/Lower Mason River Formation is shown in Figure 10. In contrast to the Smoking Hills Formation samples, there is a relative consistency in abundance among the major mineral phases. Note that quartz is combined with cristobalite, plagioclase feldspar with K-feldspar, and phyllosilicate and sulphate minerals are each summed separately. The individual minerals plotted against depth are shown in Figure 11. In general, there are no major variations in abundance with depth.

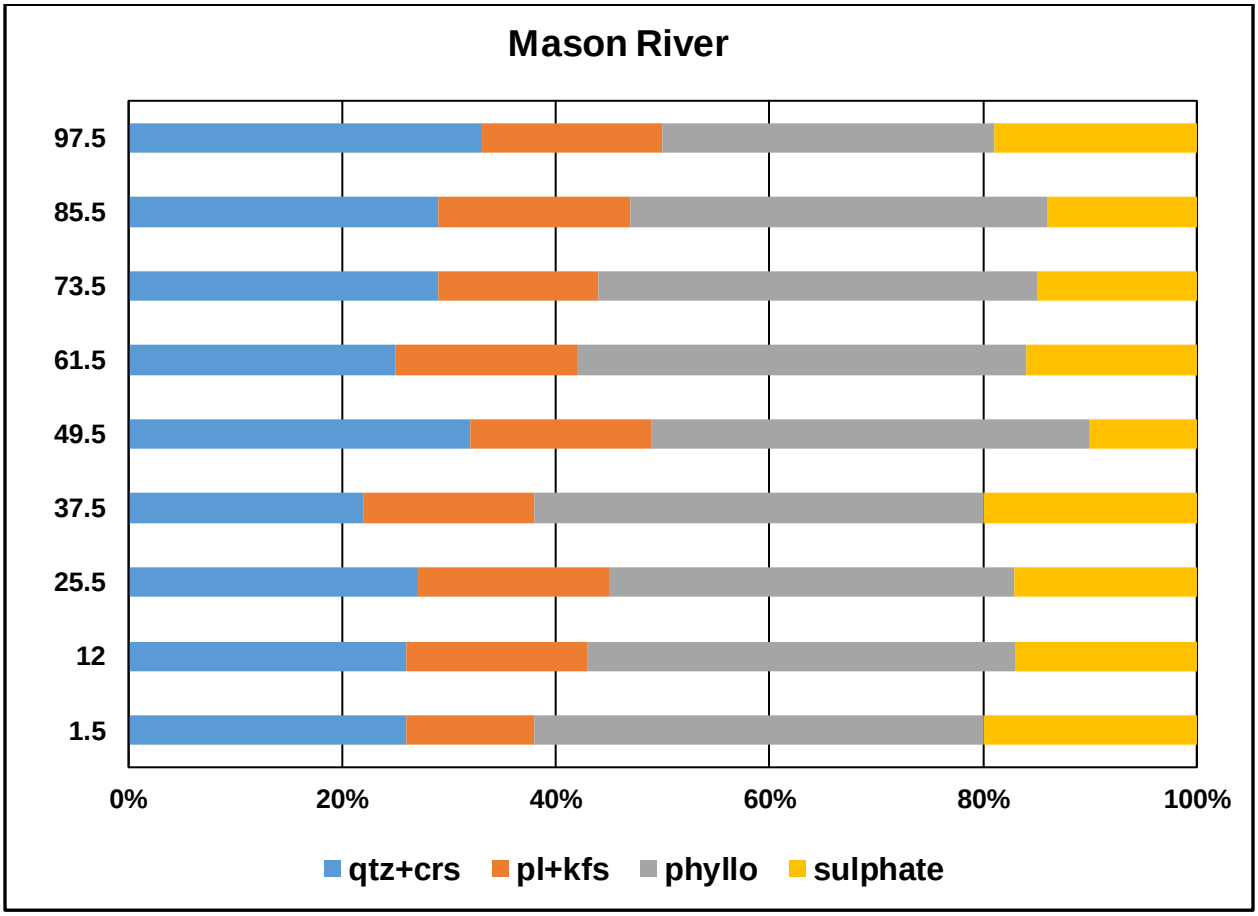

Fig. 10. Plot of major silicate minerals vs. depth (metres above base of formation) for mudstone samples from the Mason River type section (N69°28'46":W126°59'20").

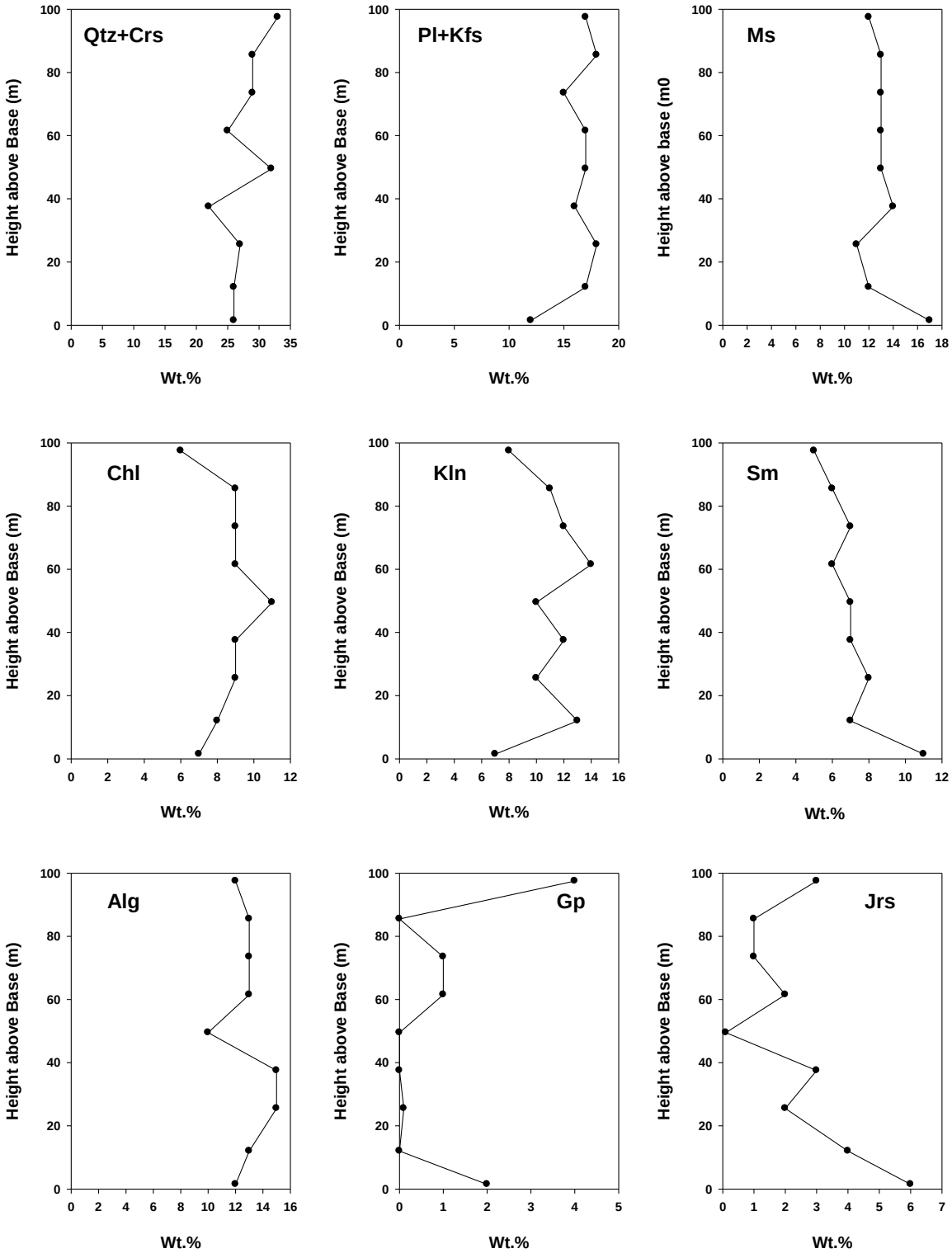

Fig. 11. Plot of major silicate, phyllosilicate and sulphate minerals vs. depth for Mason River mudstone samples.

3.4 Miscellaneous Mudstone Samples

The KUS suite (Table 4) were 4 mudstone samples from the Smoking Hills Formation that had been soaked for 30 minutes in distilled water to observe the influence on water geochemistry. The samples are dominated by hydronium jarosite (designated as Jrs-H) with minor quartz, mica and gypsum. One sample (KUS B) contains abundant plagioclase feldspar. The concretion from the bedrock raft is 100% gypsum.

3.5 Klinker Samples

Whole rock mineralogy of 19 klinker samples from the Smoking Hills area is given in Table 6 with summary statistics in Table 7. Most samples contain jarosite (combined phases; n = 16; mean = 39 wt.%), quartz (n = 17; mean = 18 wt.%) and gypsum (n = 15; mean = 13 wt.%). The remaining samples (from n = 2 to n = 12) have variable amounts of cristobalite, plagioclase feldspar, heulandite, indialite, muscovite, alunite, alunogen, bassanite and hematite. Sample GQA 18-23 is composed of 100% gypsum and Klinker 2 is composed of 100% sulphur. Barite, ferrihydrite, and tamarugite each occur in only one sample. Smectite and mixed-layer clay minerals are present in trace amounts in two samples. The goodness of fit is good with a mean of 2.4, but the samples tend to be highly amorphous, with an average crystallinity of 50 wt.% (range from 36 to 95 wt.%). The mineralogy of these klinker samples support findings of Mathews and Bustin (1984). In addition, Michel and van Everdingen (1987) report jarosite precipitating from acidic Fe-bearing seeps near Tulita, NWT, located about 54 km SE of Norman Wells. They indicated that the jarosite forms due to the encounter of groundwater with a sulphide-bearing horizon, thus forming one of the largest occurrences of jarosite in Canada.

3.6 Bocanne Samples

The physical characteristics of the 21 bocanne samples collected are provided in Table 8. The information provides their colour textural traits (e.g., needles, specks) for two samples. The yellow samples, in general, do contain native sulphur, but other colours recorded are not obviously related to a particular mineral. Semi-quantitative mineralogy is given in Table 9 with summary statistics for major phases in Table 10. The mineralogy of these samples is very complex. Based on XRD analyses, 13 different sulphate minerals were identified, often present in major to minor amounts. The presence of mineral oil used to preserve the samples (saturated) did complicate the analyses. Figure 12 illustrates the XRD pattern of the isolated mineral oil with respect to one of the samples, GQA 18-04C. This sample contains subordinate halotrichite, hexahydrite, mikasaite and millosevichite, as well as minor to trace quartz. Composition of these phases is provided in Table 1. The most common sulphate mineral present (in 16 samples) is from the halotrichite-pickeringite group (mean = 46 wt.%). Quartz was detected in 14 samples (mean = 26 wt.%) and cristobalite and native sulphur in 9 (mean = 14 wt.% and 24 wt.%, respectively). The sulphate minerals detected by XRD are scattered among the different samples.

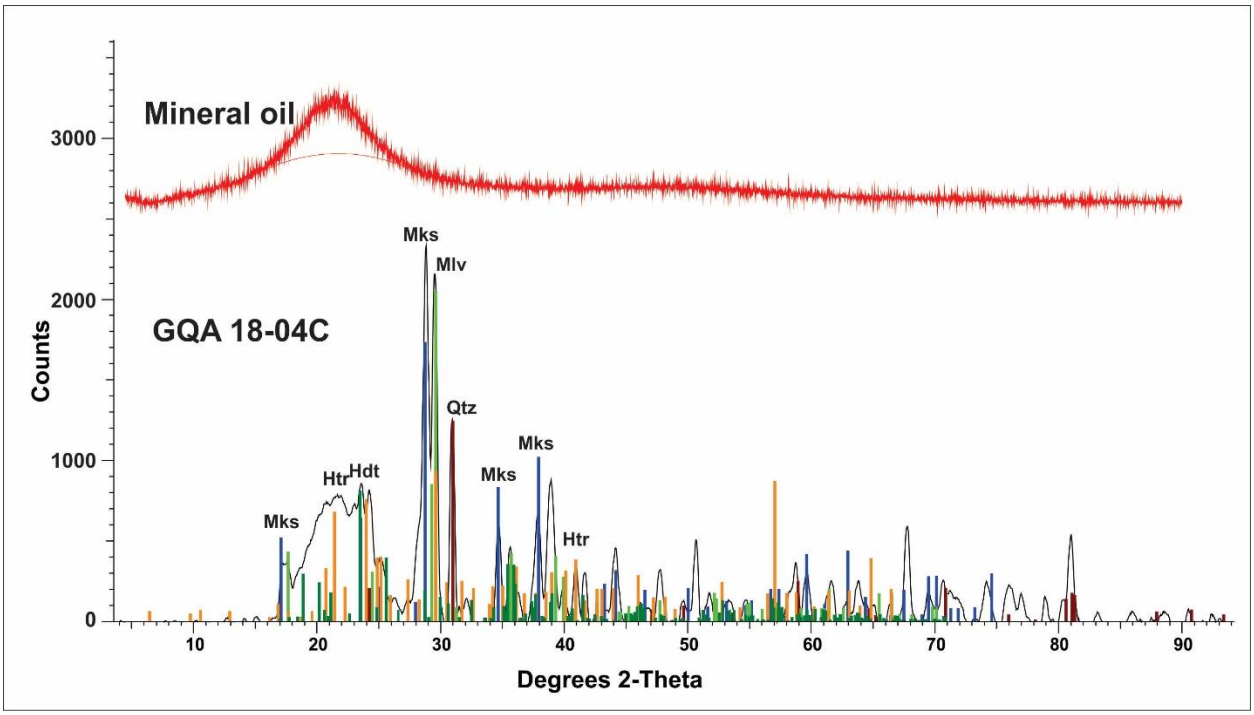

Fig. 12. Comparison of diffratograms for mineral oil used to preserve bocanne samples and sample GQA 18-04C (Htr: halotrichite, Hdt: hexahydrite, Mks: mikasaite, Qtz: quartz).

Following treatment to remove the oil a few new minerals were detectable (Table 11). Most notably native selenium was detected in four samples, and alunite, natroalunite, bassanite, mikasaite, kieserite, siderotil, steklite, voltaite, magnesiovoltaite and native sulphur were found in other samples. These likely occur in trace amounts as they were not initially detected using XRD analyses. Siderotil is from the chalcanthite mineral group that can form by dehydration of melanterite. Detailed microscopic (both binocular and SEM) analyses were performed on many of the bocanne samples. A series of photomicrographs are provided in Figs. 13-21, with a summary list in Table 12. These photomicrographs capture these rare minerals in terms of their colour (binocular) and texture (binocular and SEM) as well as their composition (EDS spectra). These images also capture the fragile nature of some of these sulphate and native minerals.

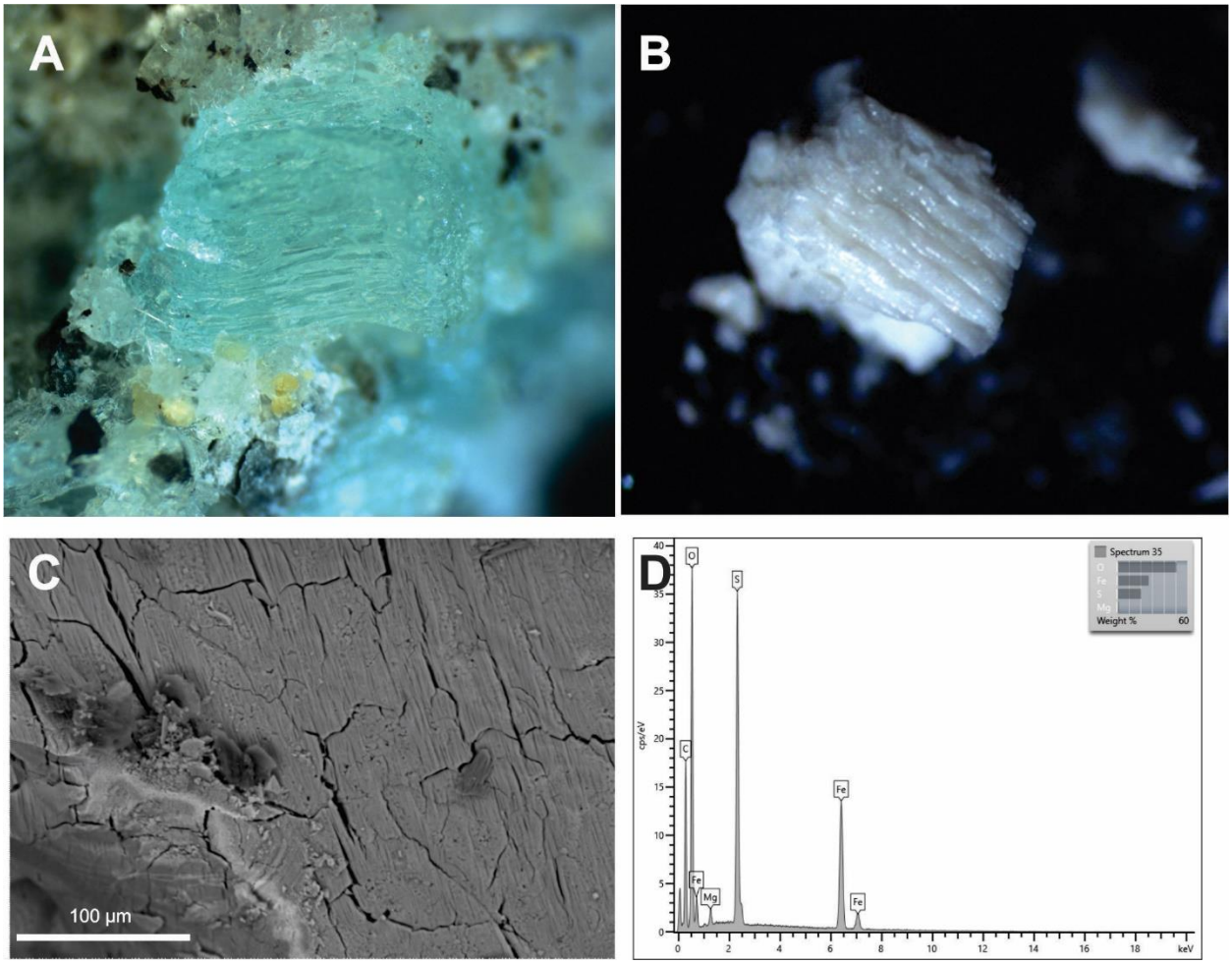

Fig. 13. Photomicrographs of melanterite from sample GQA 18-22B: A) Sample in fine layer of mineral oil (field of view (fov) ~ 2 cm); B) Oil removed and sample left to dehydrate for a week, likely siderotil (chalcanthite group; fov ~ 2 cm); C) SEM image of crystal (SEM-BSI); D) SEM-EDS spectrum of melanterite.

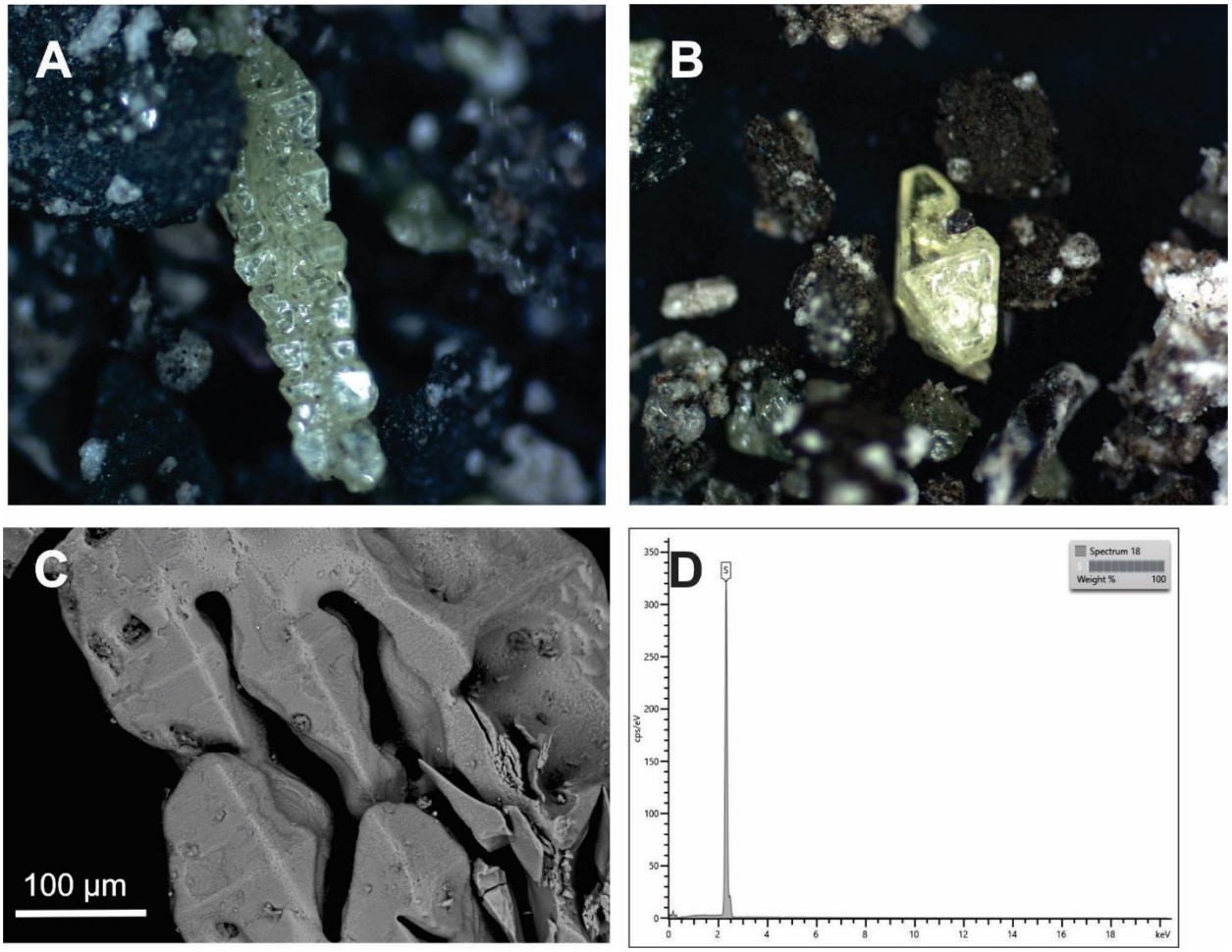

Fig. 14. Photomicrographs of native sulphur in sample GQA 18-01B: A), B) Binocular images, oil removed (fov ~ 2 and 2.5 cm, respectively); C) SEM image of sulphur crystal (SEM-BSI); D) SEM-EDS spectrum of sulphur.

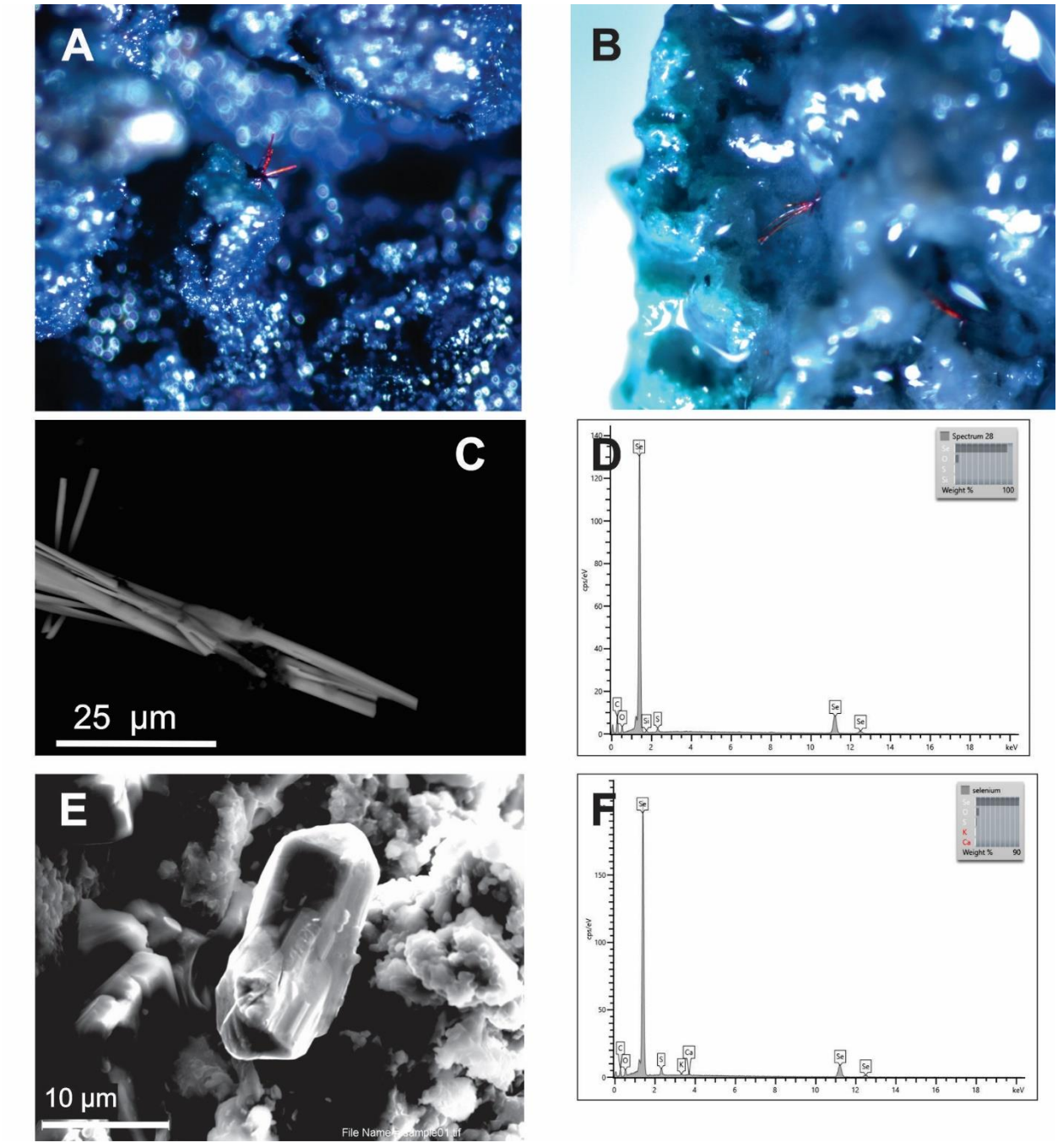

Fig. 15. Photomicrographs of native selenium: A) Needles of selenium (red) on millosevichite covered with fine layer of mineral oil, sample GQA 18-02B (fov ~ 1 cm); B) Needles in oil on millosevichite with green steklite crust, sample GQA 18-02B (fov ~ 1.4 cm); C) SEM-BSI of selenium needle, sample GQA 18-02B; D) SEM-EDS spectrum for sample GQA 18-02B; E) SEM-SEI of selenium grain, sample GQA 18-04C; F) SEM-EDS spectrum for sample GQA 18-04C.

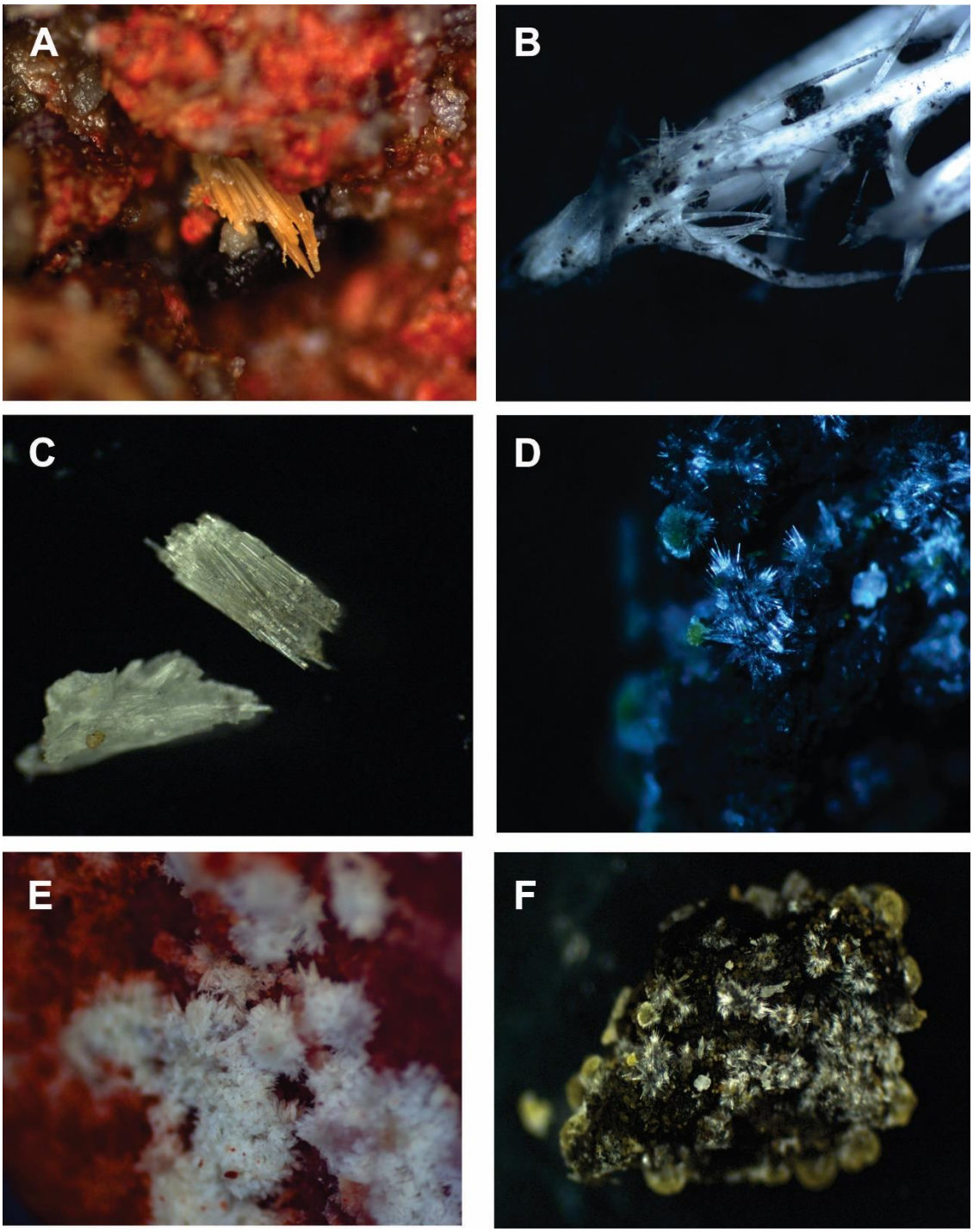

Fig. 16. Optical photomicrographs of halotrichite/pickeringite: A) GQA 18-01A, in fine layer of mineral oil (fov ~0.5 cm); B) GQA 18-01B, oil removed, pickeringite (fov ~0.4 cm); C) GQA 18-22C, oil removed, halotrichite (fov ~ 0.5 cm); D) GQA 18-22C, oil removed, clear halotrichite and yellow alunogen on black substrate (fov ~ 0.1 cm); E) GQA 18-04F, oil removed, halotrichite on hematite and quartz (fov ~ 0.2 cm); F) GQA 18-22C, oil removed, white halotrichite and yellow alunogen on black substrate (fov ~ 0.3 cm).

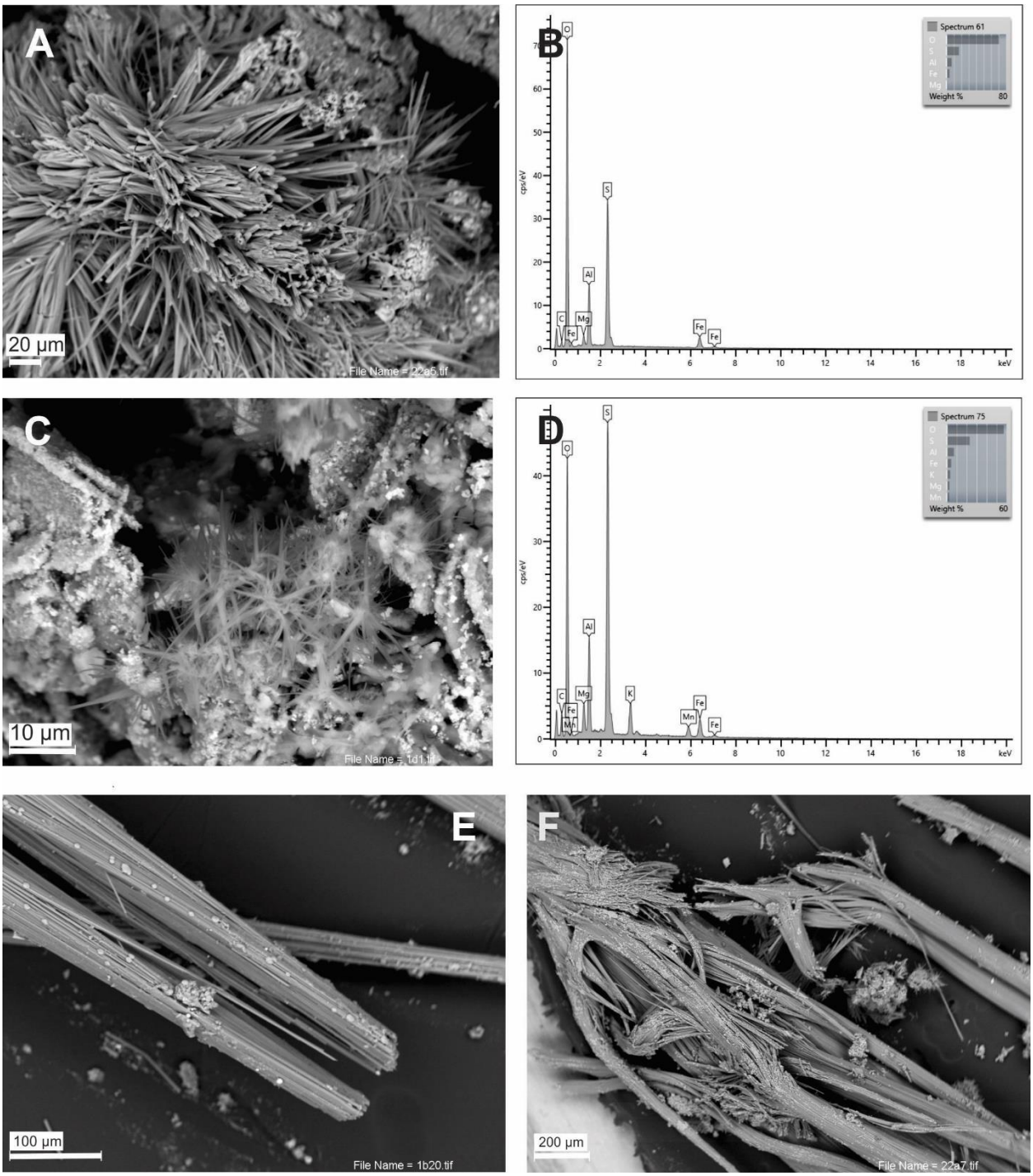

Fig. 17. SEM photomicrographs of halotrichite/pickeringite. A) GQA 18-01B, SEM-BSI of halotrichite; B) GQA 18-01B, SEM-EDS spectrum; C) GQA 18-01D, SEM-BSI of acicular halotrichite surrounded by steklite plates (SEM-BSI); D) GQA 18-01D, SEM-EDS spectrum; E) GQA 18-01B, SEM-BSI of pickeringite; F) GQA 18-01B, SEM-BSI of pickeringite.

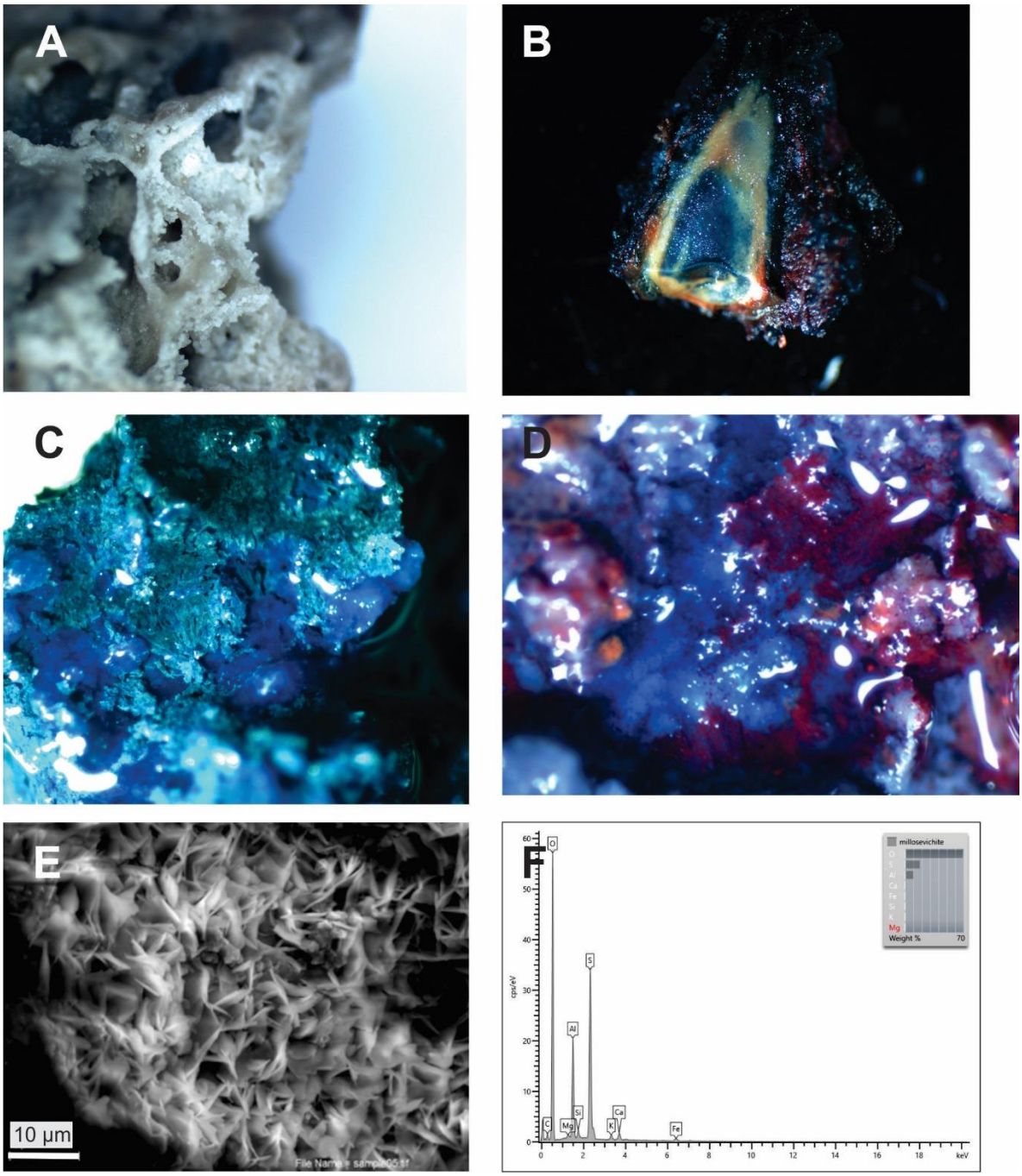

Fig. 18. Photomicrographs of millosevichite. A) GQA 18-04G, oil removed, fine grained, porous texture (fov ~ 2cm); B) GQA 18-01D, oil removed once with oil wicking to surface from internal pore space, stalactite form with concentric mikasaite (red) and millosevichite (blue-beige) (fov ~ 3.5 cm); C) GQA 18-02B, layer of oil on sample, crust of steklite (green) overlaying millosevichite (blue fov ~1 cm); D) GQA 18-04C, layer of oil on surface, crust of mikasaite (red) growing over millosevichite (blue; fov ~ 0.5 cm); E) GQA 18-04D, SEM-SEI of millosevichite crystals; F) GQA 18-04D, SEM-EDS spectrum of millosevichite.

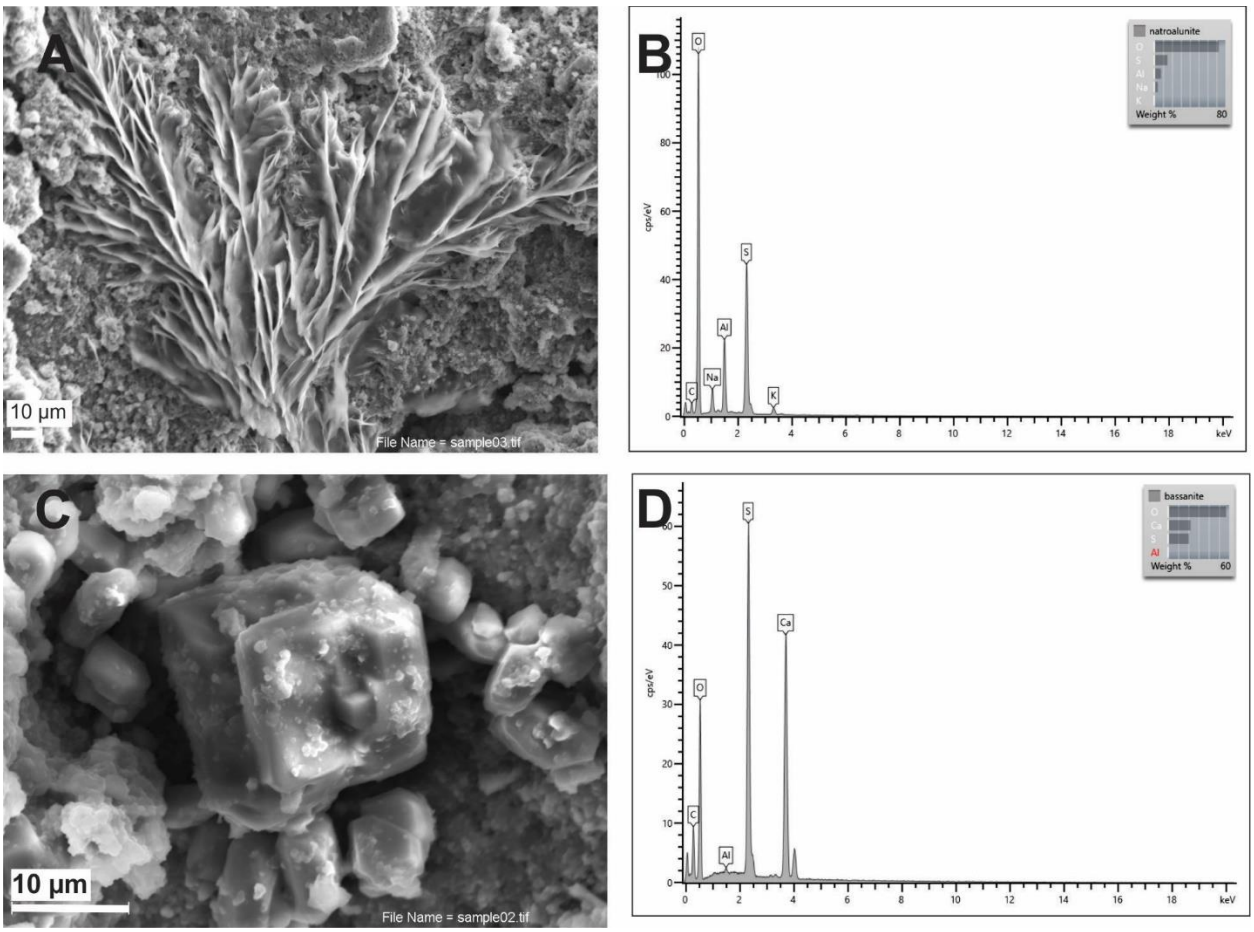

Fig. 19. Photomicrographs of various minerals from bocanne samples: A) Natroalunite from sample GQA 18-04D (SEM-BSI); B) EDS spectrum for natroalunite; C) Bassanite from sample GQA 18-04C (SEM-BSI); D) EDS spectrum for bassanite.

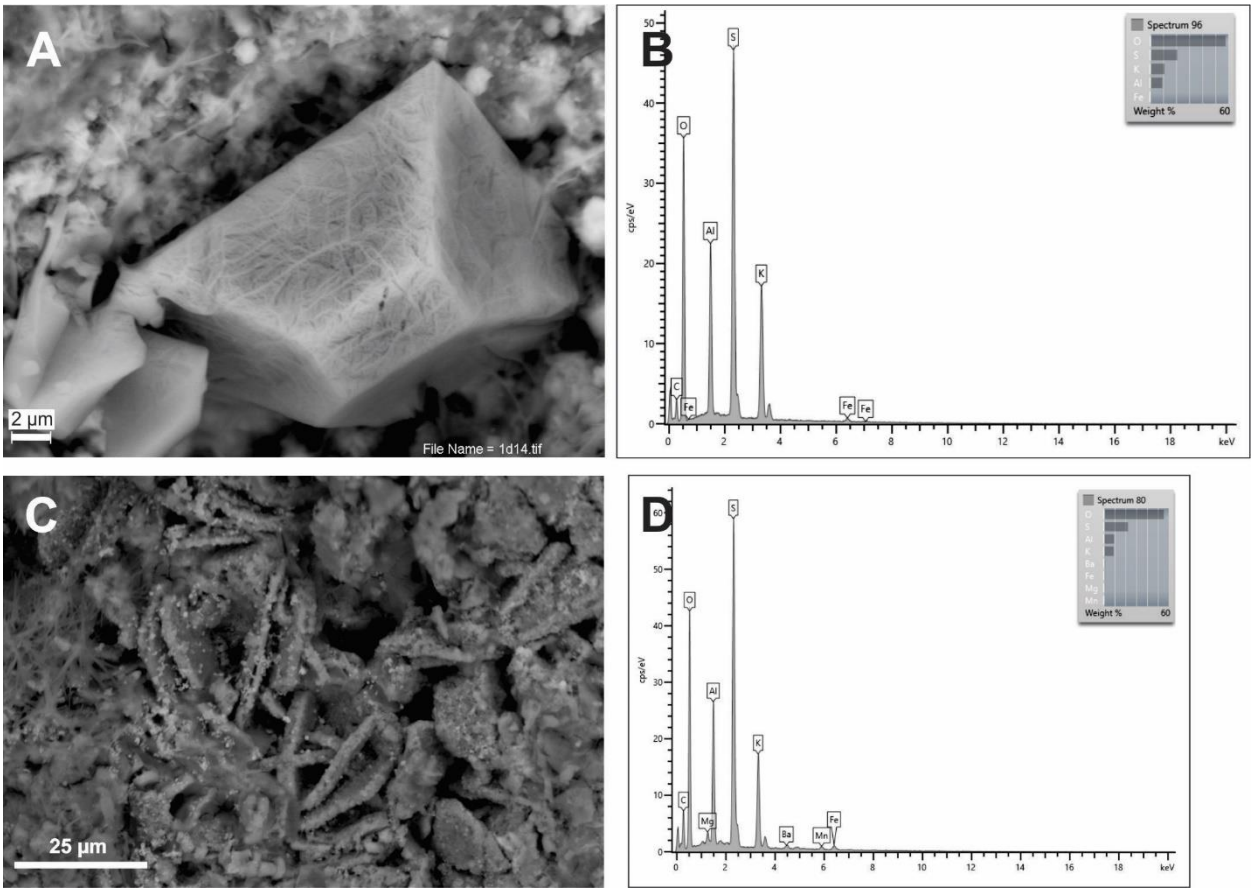

Fig. 20. Photomicrographs of steklite crystals: A), C) SEM-BSI of steklite, sample GQA 18-01D; B), D) EDS spectra for the respective steklite crystals.

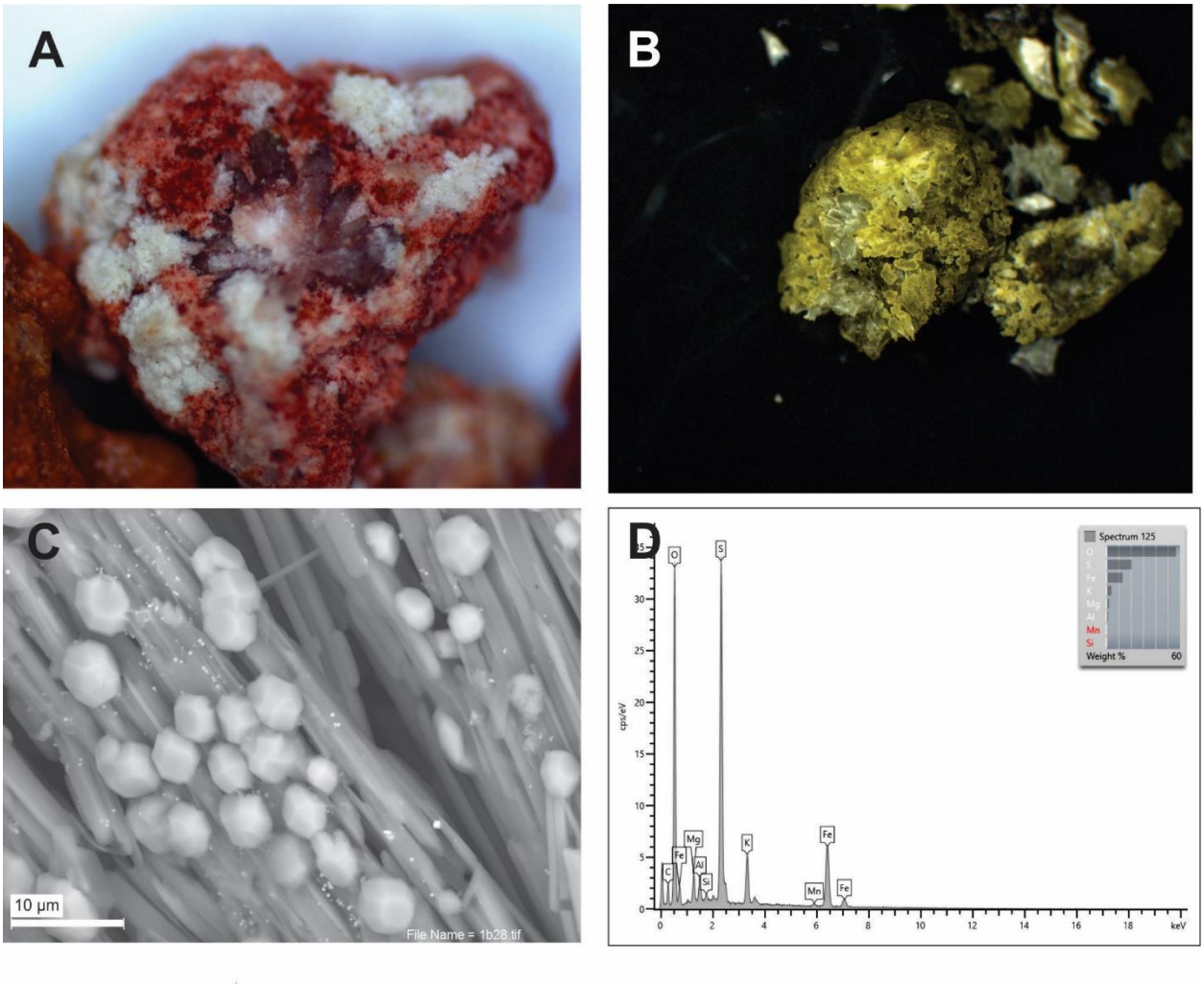

Fig. 21. A) Sample GQA 18-04F, oil removed, white halotrichite on grey quartz and hematite (fov ~ 0.5 cm); B) Alunite and natroalunite with white halotrichite, oil removed, sample GQA 18-22C (fov ~ 0.5 cm); C) SEM-BSI of voltaite/magnesiovoltaite on halotrichite needles, sample GQA 18-01B; D) EDS spectrum of magnesiovoltaite, sample GQA 18-01B.

4. SUMMARY

In all, 80 samples were analysed for their whole rock mineralogy by XRD analyses. The suites were mudstone, klinker and bocanne samples collected from the Smoking Hills area, NWT. The active bocanne sites are comprised of variable amounts of sulphate minerals whereas the inactive klinker sites are characterized mainly by jarosite, gypsum and quartz. The mudstone mineralogy is variable but most samples contain abundant to minor amounts of quartz, muscovite/illite, heulandite and jarosite. Understanding the mineralogy of these sites provides new insights on formation of high-temperature acid minerals. More research is required to tease out the changes in mineralogy of the bocanne samples, collect and preserve unaltered samples, and to verify the presence of other trace minerals.

5. ACKNOWLEDGEMENTS

This study was funded under Natural Resources Canada's Geo-Mapping for Energy and Minerals Program. It was supported by the Paulatuk and Tuktoyaktuk Hunters and Trappers committees, and operated under Inuvialuit Land Administration Licence ILA17TO-028, and NWT Scientific Research Licence 16210. This mineralogy study was completed under the Lab Study Agreement (LSA-19-4-025) for Mineralogy and Physical Properties (MPP) lab network. Special thanks to Miriam Wygergangs (GSC-Sedimentology Lab) for processing of some samples and to Isaac Fardy (Carleton University, mineralogy lab intern) for assistance with formatting and editing. We acknowledge additional sample collection by Drs. Jennifer Galloway and Manuel Bringué (GSC-Calgary) who worked with Dr. Stephen Grasby during the 2018 field campaign.

6. REFERENCES

Crickmay, C. H., 1967. A note on the term bocanne. American Journal of Science, v. 265, no. 7, p. 626-627.

Dawson, G. M., 1881. Report on the exploration of Port Simpson on the Pacific coast to Edmonton on the Saskatchewan, embracing a portion of the northern part of British Columbia and the Peace River country, 1879. Geological Survey of Canada, Report of Progress 1879-1880, Part B, p. 1-142.

Evans, D.J.A., Smith, I.R., Gosse, J.C., and Galloway, J.M., In press. Glacial landforms and sediments (landsystem) of the Smoking Hills area, Northwest Territories, Canada: Implications for regional Pliocene – Pleistocene Laurentide Ice Sheet dynamics. Quaternary Science Reviews.

Mathews, W.H. and Bustin, R.M., 1984. Why do the Smoking Hills smoke? Canadian Journal of Earth Sciences, v. 21, p. 737-742.

Michel, F.A. and van Everdingen, R.O., 1987. Formation of a jarosite deposit on Cretaceous shales in the Fort Norman area, Northwest Territories. Canadian Mineralogist, v. 25, p. 221-226.

Richardson, J., 1828. Narrative of the eastern detachment of the expedition. *In* Sir J. Franklin (ed.),

Narrative of a Second Expedition to the Shores of the Polar Sea in the Years 1825, 1826, 1827. John Murray, London, p. 187-283.

Selwyn, A. E. C., 1877. Report on exploration in British Columbia. Geological Survey of Canada Report on Progress 1875-1876, p. 28-86.

Smith, I.R., Bringué, M., Bryant, R., Evans, D.J.A., Galloway, and Grasby, S.E. (eds.), 2018. Multidisciplinary study of Cretaceous, Neogene, and Quaternary stratigraphy, and bocannes and their associated mineralogy and hydrochemistry, Smoking Hills, Northwest Territories. GEM-2 Western Arctic Project, Report of Activities 2018. Geological Survey of Canada, Open File 8482, 40 pp.

Yorath, C. J., and Cook, D., 1981. Cretaceous and Tertiary stratigraphy and plaeogeography, northern Interior Plains, District of Mackenzie. Geological Survey of Canada, Memoir 398,76 pp.

Yorath, C. J., Balkwill, H. R., and Klassen, R. W., 1975. Franklin Bay and Malloch Hill map-areas, District of Mackenzie. Geological Survey of Canada, Paper 74-36, 42 pp.